Chapter 6

Solar Cell Efficiency Increase at High Solar Concentration, by Thermionic Escape via Tuned Lattice-Matched Superlattices

A.C. Varonides

Additional information is available at the end of the chapter

http://dx.doi.org/10.5772/59039

1. Introduction

General p-i-n solar cell structures are suitable hosts for regions where quantum effects might occur; excess photo-carriers can be developed in quantum traps (quantum wells) grown along the direction of the cell (from p to n region). The cell absorbs at two different wavelengths (a) the host **($E_{host}=hc/\lambda_{host\ band\text{-}gap}$)** and (b) the optical gap wavelength (**$E_{solar\text{-}photon}=hc/\lambda_{optical\ gap}$**). The optical gap of the superlattice can be tuned to desired solar photon energy values (e.g. 1eV photons, Figure-1), with optical gap matching the desired solar photon flux (Figure 1) [1].

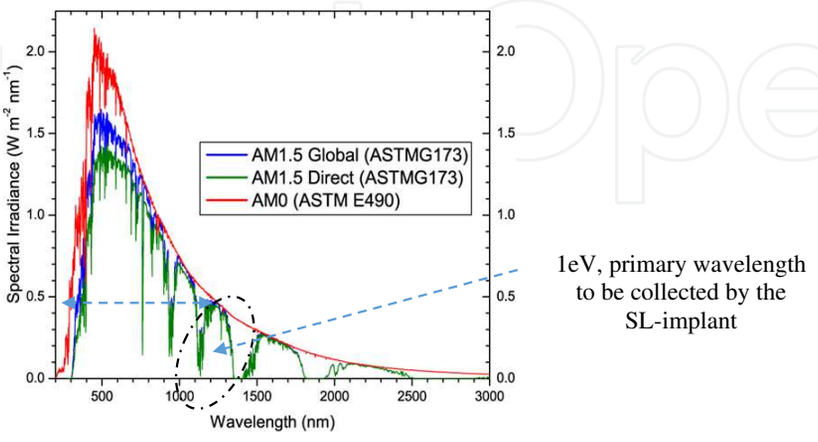

Figure 1. Solar spectrum (AM1.5 Direct) and the region of interest at primary wavelength 1240nm.

Superlattices (large number of periods with thin quantum wells) in the intrinsic region of p-i-n cells provide photo-carrier separation (electron-hole pairs or EHP's) via carrier drifting, leading to effective mass separation of photo-carriers and recombination loss reduction; the advantage of using quantum wells in the intrinsic region of the host material (here GaAs) is the widening of the gap of low-gap material (here Ge); the optical gap ($E_{e1} - E_{hh1}$) [4] caused by the narrow gap layer in the cell, can in essence be tuned to equal-energy incident solar wavelengths. This means that excess carriers may be trapped in quantum wells and thus thermionic escape will lead to *excess* currents in the cell. A cell design that could lead to excess current may occur in an all-GaAs p-i-n cell with a lattice-matched GaAs-Ge superlattice, grown in the middle of the intrinsic region (Figure 2b), and where excess photo-electrons are *thermionically* reaching the conduction band and are swept away by the built-in electrostatic field. In this chapter we provide a first-principles derivation of excess thermionic current, after radiative recombination losses are taken into account. We propose a short superlattice implanted in the middle of a bulk p-i-n solar cell (Figure 2a), with the expectation of excess current generation via concentrated optical illumination. Such a superlattice will be expected to trap photo-carriers with the chance of overcoming the potential barrier. Once such carriers are out of the quantum traps, they will be likely to join the flux of bulk currents in the p-i-n device. These carriers will essentially be swept away by the built-in electrostatic field, especially in the mid-region of the structure.

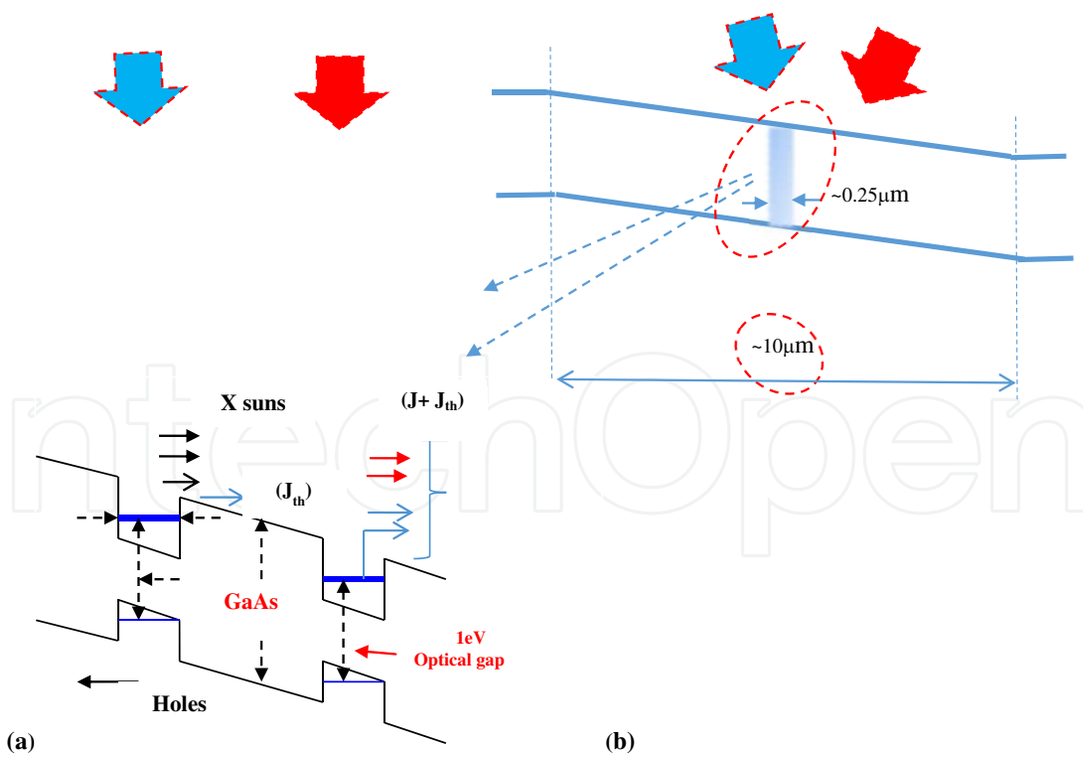

Figure 2. a) A portion of a superlattice embedded in the intrinsic region and illuminated at X suns. Carriers are excited in the quantum wells and thermionically escape to the conduction band (b) Bird's eye view of the intrinsic region with the SL (0.5 μm) portion illuminated at concentrated light.

http://dx.doi.org/10.5772/59039

2. Theory

In this section we derive thermionic currents for a single quantum well. The model as shown in Figure 1 includes a double heterostructure with a quantum well formed by a low-gap medium. According to this figure, electrons may be trapped in eigen-states in the quantum wells under both dark or illumination conditions (as long as incident photons have sufficient energy to excite carriers from the valence band to the conduction band). Once in the quantum well, electrons may thermionically acquire energy to overcome the potential barrier ΔE_c, formed by the wide-gap medium. The potential barrier is the conduction band difference $E_{c2} - E_{c1}=\Delta E_c$ (Fig-2) of the two layers that are in contact. Standard thermionic emission models [2, 3] describe thermal currents due to electrons having sufficient kinetic energy (KE) to overcome the highest conduction band edge E_{c2} ($KE=E-E_{c2} \geq \Delta E_c$) [3]. Thermionic currents can be described by integrating over all energies above E_{c2} through the following expression:

$$J = q\int dEg(E)f(E)v(E) \tag{1}$$

Where q is the electronic charge, g(E) is the electronic density of states (DOS) (eV^{-1} cm^{-3}) of the two-dimensional system (here a quantum well of width L_w), f(E) is the Fermi-Dirac distribution function, and v(E) is the velocity acquired by the escaping electrons to overcome the barrier potential. Expression (1) is usually re-written as

$$J = q\int_{Ec2}^{\infty} dE\left(\frac{m^*}{\pi\hbar^2 L_W}\right)\left(e^{-(E-E_F)/kT}\right)\left(\frac{2}{m^*}\right)^{1/2}(E-E_{C2})^{1/2} \tag{2}$$

Where the two-dimensional DOS was used for quantum wells of width L_w [3], and where the Fermi-Dirac distribution was replaced with a Maxwell-Boltzmann ($E-E_{c2} >> 3kT$). Expression (2) can be written as:

$$\begin{aligned} J &= \frac{q\sqrt{2m^*}}{\pi\hbar^2 L_W} e^{-(E_{C2}-E_F)/kT}\int_{E_{C2}}^{\infty} dE(E-E_{C2})^{1/2} e^{-(E-E_{C2})/kT} \\ &= \frac{q\sqrt{2m^*(kT)^3}}{\pi\hbar^2 L_W} e^{-(E_{C2}-E_F)/kT} \end{aligned} \tag{3}$$

The latter expression can be written in a more familiar form, in terms of the barrier height ΔE_c, which is a distinct property of the superlattice geometry. The exponential term does not change if we add and subtract the lower conduction band E_{C1}. Since

E_{C2}-E_F=(E_{C2}– E_{C1})+(E_{C1}–E_F), we can repeat (3) as follows:

$$J = \frac{q\sqrt{2m^*(kT)^3}}{\pi\hbar^2 L_W} e^{-(E_{C2}-E_{C1})/kT} \times e^{-(E_{C1}-E_F)/kT} \tag{4}$$

The last term in (4) is directly related to the total carrier concentration of electrons n_{tot} in region 1 which is the low-gap medium, hence it can be expressed via the conduction band effective density of states N_c (cm^{-3}) and the carrier density according to the standard relation

$$n_{tot} = N_C e^{(E_{C1}-E_F)/kT},$$

with

$$N_C = 2\left(\frac{2\pi m^* kT}{h^2}\right)^{3/2}$$

Implementing the latter in the current, as in (4), we obtain a finalized form of thermionic current due to thermally escaping electrons from individual quantum wells:

$$\begin{aligned} J &= \frac{q\sqrt{2m^*(kT)^3}}{\pi\hbar^2 L_W} e^{-(E_{C2}-E_{C1})/kT} \times \left(\frac{n_{tot}}{N_C}\right) \\ &= \left(\frac{qh}{m_o}\right)\left(\frac{n_{tot}}{\mu L_W}\right) e^{-\Delta E_C/kT} \end{aligned} \tag{5}$$

Where we replaced the effective mass m* with the product of rest electron's mass m_o and a numerical factor μ [$m_{c=}(9m_l m_t^2)^{1/3}$, the DOS effective mass] that differs from material to material [4]. The prefactor (qh/m_o) in (5) is a constant (q for the electronic charge, h for Planck's constant and m_o for the electron's rest mass) equal to *1.1644 x 10*$^{-22}$ ($A \cdot m^2$); the current becomes:

$$J = 1.1644 \times 10^{-22} \times \left(\frac{n_{tot}}{\mu L_W}\right) \times e^{-\Delta E_C/kT} (A/m^2) \tag{6}$$

Expression (6) describes thermionic current produced from a quantum well; this current is a strong function of (a) quantum well width (b) barrier height and (c) total carrier density in the well-layer. Total carrier concentration in the well is the sum of (a) dark carrier concentration in the quantum well n_{qu} and of (b) excess photo-carrier concentration in the miniband under illumination, δn_{ph}: $n_{tot}=n_{qu}+\delta n_{ph}$.

Hence,

$$J = \frac{1.1644 \times 10^{-22}}{\mu L_W} \times (n_{qu} + \delta n_{ph}) \times e^{-\Delta E_C/kT} (A/m^2) \tag{7}$$

http://dx.doi.org/10.5772/59039

The term n_{qu} represents carriers trapped in quantum wells [6]:

$$n_{qu} = \frac{m^*(kT)}{\pi\hbar^2 L_W} \ln\left(1 + \exp(-\frac{E_1 - E_F}{kT}\right) \tag{8}$$

E_1 is the lowest eigen-state included (suitably thin layers will provide only one eigen-solution in the wells). If the energy difference ($E_1 - E_F$) is much greater than kT, the dark quantum well contribution is essentially (numerically) negligible compared to excess photo-concentration, as seen from (8). The n_{qu} term would become significant if the Fermi level stays near the conduction band edge of the low-gap semiconductor; however this would require relatively high n-type doping levels of the quantum trap material, and hence scattering and increased absorption losses. The goal here is to embed a superlattice region in the intrinsic part of the p-i-n cell, with undoped (or low doping level) quantum well layer to reduce scattering. On the other hand, illumination would excite electrons from the valence to the conduction band at wavelengths near the gap of the layer. The quantum-well semiconductor is tuned to photons of equal energy and tuned photo-excitation populates the energy band with excess electrons δn_{ph}; these electrons can be found from the form:

$$\delta n_{ph} = n_o e^{-x/L_n} + \sqrt{\frac{\Phi_\lambda}{B}} e^{-\alpha x/2} \tag{9}$$

Relation (9) is the solution of the diffusion equation [7], describing minority photo-electrons induced in quantum wells under illumination (through Φ_λ). The first term in (9) is a diffusion term in the x direction, with electron diffusion length L_n (the solution of the homogeneous diffusion equation) and the second term includes directly the absorption coefficient in the exponential term and indirectly through the generation rate term Φ_λ; B is the coefficient of radiative recombination B respectively. More specifically, if the solar photon flux ($cm^{-2}\ s^{-1}$) is $F_{ph}(\lambda)$, the photon generation rate ($cm^{-3}\ s^{-1}$) is taken to be: $\Phi_\lambda(cm^{-3}s^{-1}) = \alpha\ (1-R)F_{ph}(\lambda)$, where R is the reflectivity of the surface and α is the absorption coefficient. At high solar concentration (e.g. X=400 or for X ≥100)), n_o, $n_{qu} << \sqrt{\frac{X\,\Phi_\lambda}{B}}$ (by at least two orders of magnitude: n_o, n_{qu} ~10^{11}-10^{12} cm^{-3}, $(X\Phi/B)^{1/2}$=10^{14} cm^{-3}), expression (7) becomes:

$$J_{ph}(A/m^2) \cong \frac{1.1644\times10^{-13}}{\mu L_W(nm)} \sqrt{X} \sqrt{\frac{\Phi_\lambda}{B}} (e^{-\alpha x/2} e^{-\Delta E_C/kT}) \tag{10}$$

Where both n_{qu} and n_o terms have been removed as negligible compared to X-sun photo-generation. On the other hand, B represents the cross section of radiation recombination losses (radiation coefficient); we use a nominal value of the order of $10^{-10}\ cm^3s^{-1}$=$10^{-16}m^3s^{-1}$ [8]. Currents in (10) depend on (a) width L_w of quantum wells (b) carrier effective mass $m^*=\mu\ m_o$ (c) solar concentration X (# of suns) (d) carrier photo-generation Φ_λ and (e) conduction band discontinuity ΔE. The formula above describes thermionic escape current from an illuminated

quantum well of width L_w (nm), with one mini-band and tuned to a specific solar wavelength λ_o. Such a choice creates favorable conditions for absorption of photons at energy E_o(eV)=1.24/λ_o(μm); one can deduce the value of carrier generation rate Φ_λ by dividing the irradiance I_{rr}(W/m^2) at the specific wavelength $\lambda_{o,}$ by the energy of the corresponding photon of energy E_o. In other words, the solar photon flux F_{ph} (m^{-2} s^{-1}) is the ratio $I_{rr} / E(\lambda_o)$. By tuning a quantum well at 1eV (see Figure-1), we increase the prospects of photon absorption at λ_o=*1.24μm* (note also that E (λ_o=*1.24μm*)=1.24/1.24=1eV), and hence the solar photon flux at λ_o is (see also Figure-1):

$$F_{ph}(\lambda_o) = \frac{I_{rr}}{E(\lambda_o)} = \frac{I_{rr}(W/m^2/nm)}{E(\lambda_o)(J/nm)} = 3.12\times10^{18} m^{-2}s^1 \quad (11)$$

Where the irradiance I_{rr} *at* a primary wavelength λ_o=*1,240.00 nm* is taken equal *to 0.5W/m*^{2} [1]. The carrier generation rate (absorption coefficient is assumed to be ~ 10^4 cm^{-1}=10^6 m^{-1}) is:

$$\Phi_{\lambda o} = \alpha(1-R)F_{ph}(\lambda_o) \cong (10^4\times10^2)\times3.13\times10^{18} m^{-3}s^1 = 3.13\times10^{24} m^{-3}s^1$$

[Note also the approximation: a 1240nm photon, impinging on a 5nm quantum well, suffers negligible reflection, hence *R negligible*]. The conduction bandgap term ΔE, is the energy discontinuity between GaAs and Ge layers. Numerical values of ΔE are strongly dependent on fabrication conditions and crystal orientation. We compromise with a well-balanced value 350 meV for ΔE [9]. Based on numerical values of the relevant parameters, the composite cell will generate excess thermionic currents at X suns and with N superlattice periods:

$$J_{ph} = 1.557N\sqrt{X}(mA/cm^2) \quad (12)$$

The exponential term $e^{-ax/2}$ in (10) refers to absorbed radiation within the span of single quantum well (several nanometers), while the absorption coefficient is taken to near 10,000 cm^{-1} [10]. This means that this exponential term will be very close to 1 within the span of one quantum well (~ 0.998) and it is not a significant term in computing expression (10). Expression (12) is now a finalized result of thermionic current density due to electrons escaping from a Ge-quantum well illuminated at a primary wavelength λ_o. Note also that we assumed no losses of thermionic carriers once they are above E_{C2} (work in progress; see also expression (3) above, in relation with Figure 2a).

To summarize, we have developed a thermionic current formula based on the following assumptions:

a. Electrons are assumed to have kinetic energy $KE \geq E_{c2} - E_{c1}$

b. Electrons occupy *2-D* states in quantum wells

c. Total current is calculated from *dj=q g(E) f(E) v(E) dE*

http://dx.doi.org/10.5772/59039

d. Fermi-Dirac statistics is approximated to Maxwell-Boltzmann's

e. Thermal currents are strong functions of incident *concentrated* solar photon radiation

f. the quantum wells are tuned at their optical gap; high concentrations of excess photo-electrons are expected to accumulate in the mini-bands and hence significant thermionic currents are expected

g. Currents depicted here, are in accordance with thermionic patterns $J \sim J_o\, e^{-q\Phi/kT}$ (Φ the potential barrier) and given by (10) as a strong function of solar concentration and number of periods.

h. We use 5nm quantum well widths (GaAs/Ge/GaAs), tuned at 1eV; the current density is

$J_{ph} = 1.557\sqrt{X}\,(mA/cm^2)$; Per low-gap layer

The figure below indicates solar thermal current dependence on solar concentration (from (11), N=1).

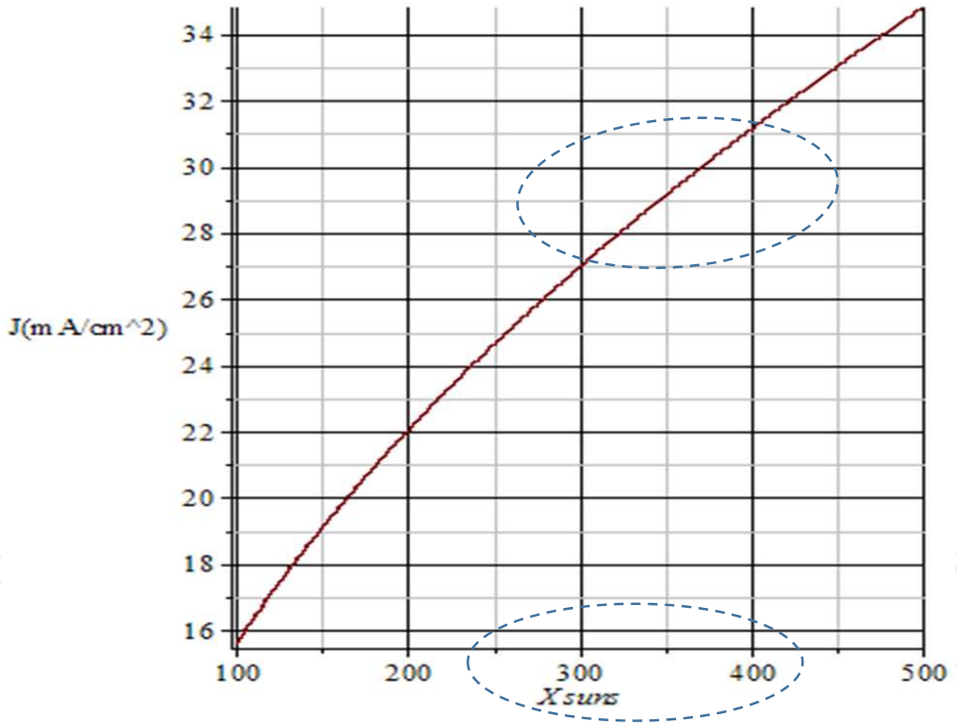

Figure 3. Thermionic current density dependence on solar concentration. 31mA/cm^2 excess thermal current is generated per quantum well at 400 suns (tuned at 1eV, $N=1$, $J \sim 1.557X^{1/2}$).

From Figure-3, we see that highly illuminated quantum well layers at specific wavelengths produce high currents (for instance, 31mA/cm^2 at 400 suns). Excess short circuit current J_{ph} increases drastically with photo-concentration as seen from Figure-3. Such rapid rise is expected (the higher the irradiance the more carriers available for thermal escape from the wells). However, drastic increase in current does not (a) affect open circuit voltage and (b) total

efficiency. Open-circuit voltage remains near the one-sun value (X=1), while fill factors reduce. As a result, the efficiency of the hybrid cell will be affected accordingly. The next section deals with the collection efficiency of the hybrid cell (bulk plus superlattice cell).

3. Device design

Incorporating a superlattice-layer GaAs/Ge, with 5nm-thick quantum wells, embedded in the middle of the intrinsic region of the bulk cell, will increase the current dramatically but not the open circuit voltage. This current will add to the bulk GaAs-related current of the PV cell, and will affect the open-circuit voltage as well. The bulk cell illuminated at X suns will produce an open-circuit voltage V_{oc}^{ph} given by the standard formula:

$$V_{oc}^{'} = V_t \ln(\frac{XJ_L}{J_o} + 1) \cong V_t \ln(\frac{XJ_L}{J_o}) = V_{oc} + V_t \ln(X) \tag{13}$$

Where the photo-current has been multiplied by the X (suns) factor [1]. Based on the above, net *OC*-voltage will increase by 15mV: V_t *ln* (X)=0.025 ln (400)=0.150V (with V_t=kT/q) and hence $V_{oc}^{(ph)}$=1.051+0.15=1.201V. We simulate a GaAs p-i-n cell with the following geometry [11]:

a. Total device 14μm)

b. Length of p-region 2 μm

c. Length of intrinsic region 10 μm

d. Longer intrinsic region provides excess photo-carriers swept away from the junctions; excess minority carriers are developed in both p-and n-regions

e. Total current is essentially the sum of minority and off-intrinsic region currents

f. Length of n-region 2 μm

g. GaAs/Ge multilayer in the intrinsic region (Ge layers at 5nm): total length of SL region for 100 periods, 100 x 5=500 nm=0.5 μm

h. Illumination of the whole device (including intrinsic region) at X suns (e.g. X=400)

i. PC1D simulations of a host-GaAs p-i-n host cell, (steps (a) through (d)) lead to J_{sc}=J_L=25.73 mA/cm^2, V_{oc}=1.051V, FF=0.94, at X=1, P_{in}=100mW/cm^2); efficiency η=(0.94) (25.73) (1.051) / P_{in}=25.42%

j. Illumination of the composite cell at X-suns will affect the collection in two ways (i) short-circuit photo-currents and input power will increase by a factor X (ii) OC-voltage will increase as indicated by (12).

k. The fill factor FF is $FF = 1 - \frac{V_t}{V_{oc}^{total}} \ln(1 + \frac{V_m}{V_t}) - \frac{V_t}{V_{oc}^{total}}$ [12]

http://dx.doi.org/10.5772/59039

1. Host (bulk) GaAs-cell (no superlattice, X=400) shows 26.26%, through FF and V_m computation

$$V_m = V_{oc}^{total} - V_t \ln(1+\frac{V_m}{V_t}) = (V_{oc} + V_t \ln X) - V_t \ln(1+\frac{V_m}{V_t}) \tag{14}$$

$$\eta = (0.85)\frac{(400\times 25.73)\times(1.201)}{400} = 26.26\%$$

Note that open-circuit voltage is $V_{oc}^{(X=400)}=V_{oc}^{(X=1)}+V_t \ln(400)=1.201V$

The efficiency of the hybrid (bulk+superlattice) device is:

$$\begin{aligned} &\eta = (FF)\frac{(XJ_L + J_{ph})}{XP_{in}}V_{oc}^{'} = (FF)\frac{J_L + (\frac{J_{ph}}{X})}{P_{in}}V_{oc}^{'} \\ &Or \\ &\eta = (FF)\frac{J_L + (1.557NX^{-1/2})}{P_{in}}V_{oc}^{'} \end{aligned} \tag{15}$$

We re-write (15) by splitting it in two parts containing bulk and superlattice regions:

$$\begin{aligned} &\eta = (FF)\frac{J_L + (1.557NX^{-1/2})}{P_{in}}V_{oc}^{'} \\ &= (FF)\frac{J_L V_{oc}^{'}}{P_{in}} + (FF)\frac{1.557X^{-1/2}V_{ov}^{'}}{P_{in}} \equiv \eta_{bulk}^{X} + \delta\eta \end{aligned} \tag{16}$$

The first term of (16) is the bulk-cell efficiency at X suns, and the second one is the excess collection efficiency due to the superlattice region. Rewriting (16) we get:

$$\eta = \eta_{bulk} + \delta\eta = \left(FF\frac{J_L V_{ov}^{'}}{P_{in}}\right) + \left(FF\frac{1.557V_{oc}}{P_{in}}N\right)(1+\frac{V_t}{V_{oc}}\ln X)X^{-1/2} \tag{17}$$

From (16), we predict total efficiency $\eta = 26.26\% + 0.079N(\%) = 28.63(\%)$ (with FF=0.85, X=400, V_{oc}=1.051V, V_t=0.025eV, N=30). On the other hand, collection efficiency at 400 suns for 50 periods will increase efficiency to 30.21%. The advantage of higher efficiency, at greater N values, is depicted in Figure 4 below:

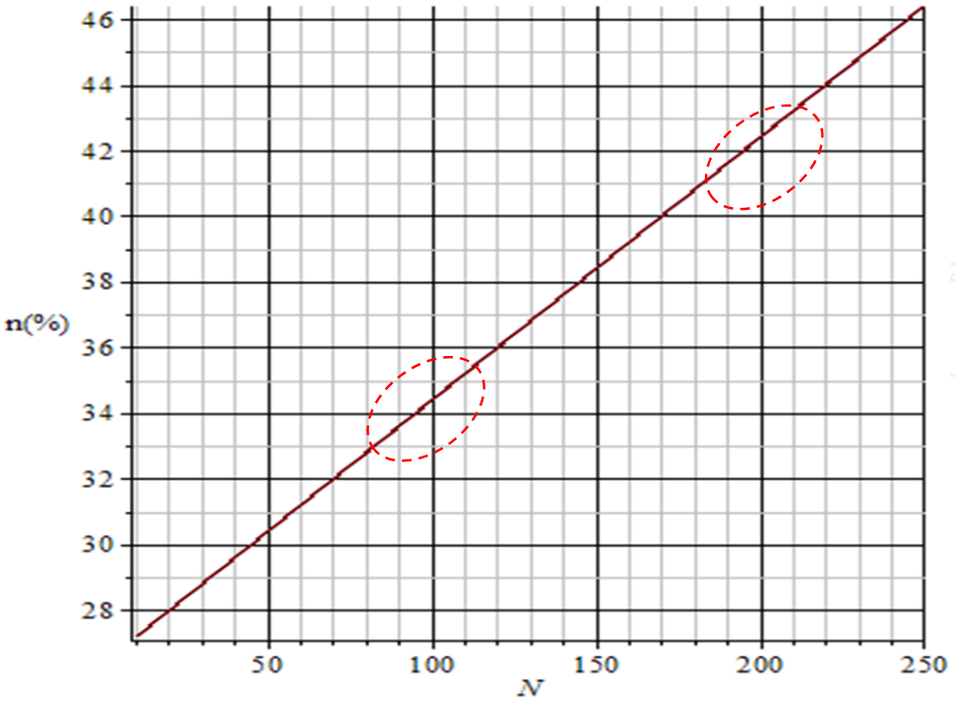

Figure 4. Collection efficiency vs number N of 5nm-Ge layers in the intrinsic region of a GaAs p-i-n cell. Note that 42% is feasible with 200 periods at 400 suns (XP_{in}=400mW/cm^2).

Note from Figure 4, that 42% collection efficiency can be expected at 400 suns and at large number of superlattice periods (N ~ 200). By using (11) in (17) we propose the total efficiency as the sum of two conclude by re-writing as the sum of two factors bulk efficiency and excess efficiency:

$$\eta(\%) = \eta_{bulk} + \delta\eta = \eta_{bulk} + (1.557FF) \times \frac{NX^{-1/2}V_{oc}^{'}}{P_{in}} \tag{18}$$

Expression (17) essentially predicts excess efficiency $\boldsymbol{\delta\eta}$ of a cell, enriched with an embedded N-period superlattice, under concentrated power equivalent to X suns. We would also like to see excess efficiency against X at a fixed N: (17) can be re-written:

$$\eta = \eta_{bulk} + \delta\eta = 26.26 + \frac{1.323(N)}{P_{in}\sqrt{X}}(V_{oc} + V_t \ln X)) \tag{19}$$

Note however from (18) that the excess efficiency δη strongly depends on $X^{-1/2}$ and N. High X "slows down" excess efficiency as shown from Figure-5:

Note from Figure-5 that high X does not necessarily mean better performance; at 100 and 400 suns, 30 SL layers in the intrinsic region will provide 30.88% and 28.63% collection respectively;

http://dx.doi.org/10.5772/59039

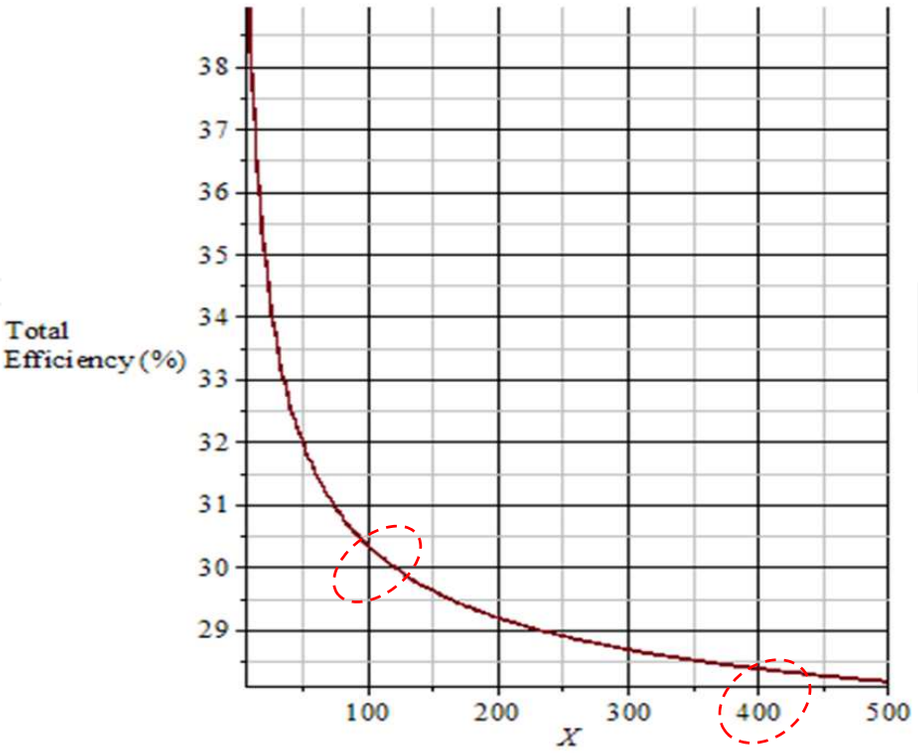

Figure 5. Efficiency vs number of suns X, with 30 superlattice layers in the intrinsic region. Excess efficiency decreases with X (see (18)). Note higher efficiencies at lower irradiances.

this is because excess efficiency gains (δη) drop quickly with X (Fig. 5 and expression (18)); high concentration does not increase the second term of (17) or (18). For instance, compromising with N=50 periods, 100 suns would suffice for excess efficiency δη=7.7% (or total efficiency of 25.50+7.7=33.20% according to (18). As the concentration increases, the excess term decreases down to the bulk cell's efficiency. On the other hand, as long as the concentration is kept between 100 and 500 suns, considerable increase in efficiency is plausible as seen in Figure 5. A summary of cell performance improvement is shown below (Table 1) where (i) bulk cell at one sun (ii) bulk cell at 400 suns and (iii) hybrid cell at 400 suns is depicted.

Table-1 summarizes some results predicted at 1 and 400 suns respectively; note (a) ideal efficiency at 400 suns with varying period number N.

Cell properties & conditions	**GaAs p-i-n cell**	**GaAs p-i-n cell (no SL)**	**Hybrid cell with GaAs/Ge superlattice (SL)**
J_L (mA/cm^2)	25.73	$400J_L$	31.14 (X = 400, N = 1)
V_{oc} (V)	1.051	1.201	1.201
FF	0.94	0.85, **[(FF) = 0.85, X > 100]**	0.85

Cell properties & conditions	GaAs p-i-n cell	GaAs p-i-n cell (no SL)	Hybrid cell with GaAs/Ge superlattice (SL)
X (suns)	1	400	400
η (%)	25.42	26.26	28.63 (N =30) 30.21 (N= 50)[16] 32.58 (N = 80) 38.11 (N 150) 42.06 (N = 200) 52.33 (N = 330)

Table 1. Bulk and hybrid cell at 1 and 400 suns (P_{in}=100mW/cm^2, X=1); The bulk p-i-n GaAs cell is simulated as a standard 1-cm^2 PV device.

Notice improvements in the efficiency of the bulk pin GaAs cell: from 25.42% (X=1) to 26.25% (X=400) and 28.63% at X=400, N=30, and 30.21% at X=400, N=50 (compare with Fig-16 of reference [16] good agreement in overall efficiency for p(GaAs)-I(quantum well)-n(GaAs) strained-layer cell).

Table-2 below summarizes improvements on cell performance:

Hybrid cell OC-voltage $V'=V_{oc}+V_t \ln X$	X(suns)	δ/N	Excessefficiency δη (%)	Bulk cell Efficiency,	Hybrid cell Efficiency [b]
1.166	100	0.154	7.70	25.50	33.20
1.183	200	0.111	5.55	25.87	31.42
1.194	300	0.091	4.55	26.11	30.66
1.201	400	0.079	3.95	26.26[a]	30.21
1.206	500	0.071	3.55	26.37	29.92

[α]: (25.73) ($V_{oc}+V_t$ lnX) (0.85)=26.26%; [b]: N=50.

(Where $\delta = \frac{1.323 V_{OC}^{'}}{P_{in}\sqrt{X}}$ (see (18)), and V_{OC} (bulk, one sun)=1.051V).

Table 2. Comparison between bulk and hybrid cell at various solar concentrations

Note that 50% efficiency is feasible by posing the question: what is the N value in the intrinsic region of the host cell at a given X? Table 3 below summarizes device design for high performance; for instance, 50% efficiency is feasible with a 1.5 μm superlattice at 400 suns. Table 3 summarizes and compares bulk and hybrid cell performance at different concentration levels. For instance, note that 50% efficiency is feasible under 300 suns with 260 Ge layers. Of course, cost reduction and high efficiency levels would lead to the obvious choice (Table-3)

http://dx.doi.org/10.5772/59039

with 100 suns illuminating a 160-period superlattice in a p-i-n GaAs cell with 10 um-long intrinsic region.

X (solar concentration)	Bulk η(%) GaAs pin cell	δη(%) GaAs-Ge (SL)	η + δη (%) Hybrid cell combined efficiency	N Number of SL periods	L_{SL}(μm) Total length of SL region	L_{SL}/L_i SL region vs i-region of control cell
100	25.50	24.50	50.00	160	0.800	8%
200	25.87	24.13	50.00	220	1.100	11%
300	26.11	23.89	50.00	260	1.300	13%
400	26.26	23.74	50.00	300	1.500	15%
500	26.37	23.63	50.00	330	1.650	16.5%
600	26.48	23.40	50.00	360	1.800	18%

Table 3. Choice of number N periods for 50% total ideal efficiency at different solar concentrations X; the last column indicates the length of the SL region (length of intrinsic region L_i=10μm); last column compares superlattice vs intrinsic region widths. We set a lowest limit of X=100 to ensure negligible dark carrier concentration (see also expression (7)). High X increases current but not necessarily the efficiency.

Table-3 above is an extrapolation to higher efficiencies, feasible through the proposed structure (Figure 6). We set a limit at 50% and simulate the feasibility of the structure proposed. The latter is a p-i-n cell with a superlattice in the middle of the intrinsic region; the superlattice is illuminated at X-suns and produces excess thermionic current density from two-dimensional systems (quantum wells). The most reasonable choice is indicated by the first row of Table-3, where 50% can be reached (X=100, N=160; η=50%). Such designs and high efficiency options are perfectly suited for concentration photovoltaics (CPV); note also that maturity of (a) current light-concentrating systems and (b) device enrichment via routine MBE growth-techniques make the proposed design reasonable for production. On the other hand, three junction cells (MJ) are equally complicated structures because they include three cells in series with highly doped AlGaAs/GaAs tunnel-junctions linking them. Our proposed cell is a bulk GaAs cell enriched with a matched N-period superlattice and without the need of any tunnel junction. The proposed device relies on the bulk properties of a GaAs cell which in turn is enriched with an implanted superlattice strip that provides excess current under X > 100. Its twofold-advantage over current multi-junction (MJ) cells is (a) absence of top cell (hence no photon shadowing effects) and (b) absence of tunnel junctions (TJ). Such a superlattice grown in the mid-intrinsic region of an all-GaAs p-i-n solar cell illuminated at X suns is depicted in Figure-6 below. Light is supposed to be focused on the interior of the device covering the superlattice where 1eV photons are expected to be strongly absorbed and from where photo-carriers are expected to thermionically escape.

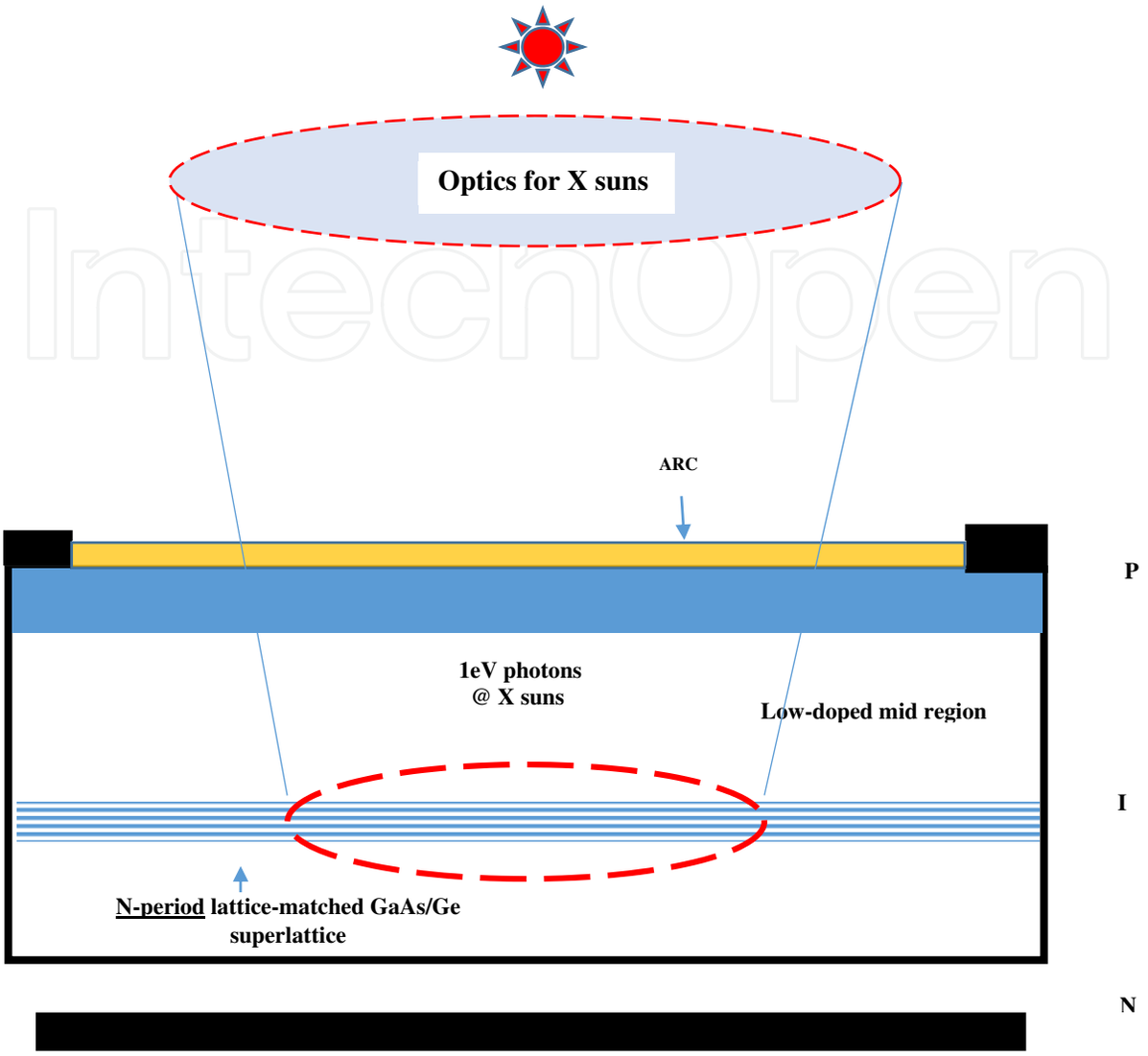

Figure 6. Concentrated solar radiation incident on a 1-cm² GaAs p-i-n cell with a GaAs/Ge lattice-matched superlattice (SL) in its intrinsic region. Total efficiency of the hybrid cell is the sum of bulk cell efficiency η and excess efficiency. Implanted SLs in the bulk are feasible based on routine MBE techniques [15]. Details of the optical system and the spot covering most of the SL region are under study.

As seen from Figure 6, a superlattice can become the source for excess carriers in the conduction band if light can be concentrated on it inside the pin cell. This is an immediate advantage: the SL region generates excess carriers and causes efficiency increase δη as seen in expression (18):

$$\delta\eta = \frac{1.323(N)}{P_{in}\sqrt{X}}(V_{oc} + V_t \ln X)$$; (No losses due to excess carrier scattering are assumed, see also [12])

Figure-6 presents the main concept: a lattice-matched superlattice in the middle of the bulk GaAs i-layer of the control cell and illuminated at X suns improves cell performance through thermionic escape of photo-electrons from individual quantum wells. In our analysis we

http://dx.doi.org/10.5772/59039

assume 100% escape rate of these electrons from their quantum traps [12] and an ideal device performance in terms of quality factors and shunt resistance.

4. Conclusions

A different type of multijunction cell structure is proposed in this chapter. The multijunction term refers to a proposed lattice-matched superlattice, grown in the bulk of the intrinsic region of a p-i-n cell; current high efficiency cells are basically designed as a top-cell/bottom-cell tandem arrangement, on GaAs or Ge. These cells are in-series connected via tunnel junctions and the whole structure is illuminated at high solar irradiance [13, 14, and 16]. We demonstrate the case for higher efficiencies achievable in GaAs p-i-n solar cells through embedded lattice-matched superlattices in the intrinsic region. Our model is based on thermionically escaping carriers from individual quantum wells of the superlattice in the intrinsic region of the p-i-n control cell. The total carrier concentration in quantum wells is the sum of (a) photo-excited carriers and of (b) carriers that occupy eigen-energy levels under dark. The total population in each quantum well is dominated by photo-carries at highly concentrated incident solar light. The latter has been the major approximation in our model, namely, the photocarrier population is much greater than the bulk and quantum well populations respectively in each and every quantum trap in the cell. We then proposed a p-i-n device that includes a superlattice structure in the middle of its intrinsic region, a superlattice layer composed of GaAs/Ge units (the low gap material is in essence the quantum well: Ge). The advantages of such a proposal are (a) concentrated light on the cell (X=400 suns) produces excess thermionically escaping carriers (b) these carriers may overcome the potential barriers of the superlattice region and contribute excess photo-current that depends strongly on concentration level X and on the number of superlattice (SL) periods N and (c) the SL region is only a small fraction of the total device length. Our results stand in good agreement with efficiency improvements of standard designs of tandem/multijunction cells. We simulate a GaAs control/reference device hosting a superlattice embedded in its intrinsic region that can generate appreciable currents at 400 suns. Specifically, a 26.26% efficient all-GaAs control solar cell (X=400) increases its efficiency to 30.21% when a 50-period GaAs/Ge-superlattice is grown in its intrinsic region. Excess collection efficiency depends on the period number of the superlattice and the concentration level. We claim that 50% efficiency levels are feasible for p(GaAs)-i(GaAs/Ge-SL)-GaAs cells with either 330 periods at 400 suns or 160 period under 100 suns. The sequence of steps for high cell performance is outlined in the figure below:

The sequence shown above describes the steps undertaken in this chapter. The control cell is the primary choice that provides the fundamental efficiency of the cell. The superlattice unit, which is a small fraction of the mid-region of the control cell, can be implanted in the cell as a lattice-matched layer. Generalizing we show that cell efficiency may increase by means of a superlattice implanted in the mid of a p-i-n GaAs cell according to the formula:

$$\eta(\%) = 26.26 + \left[(N)(W) \frac{1.323(V_{OC} + V_T \ln(X))}{P_{in}\sqrt{X}} \right]; X \geq 100 suns$$

Where N is the superlattice number of periods, W is the probability of excess carriers being collected [12], P_{in} is the incident solar power, V_T is the thermal voltage. The proposed design is ideal for concentrated photovoltaics (CPV): small size cells (therefore reduced material costs) and low-cost optics.

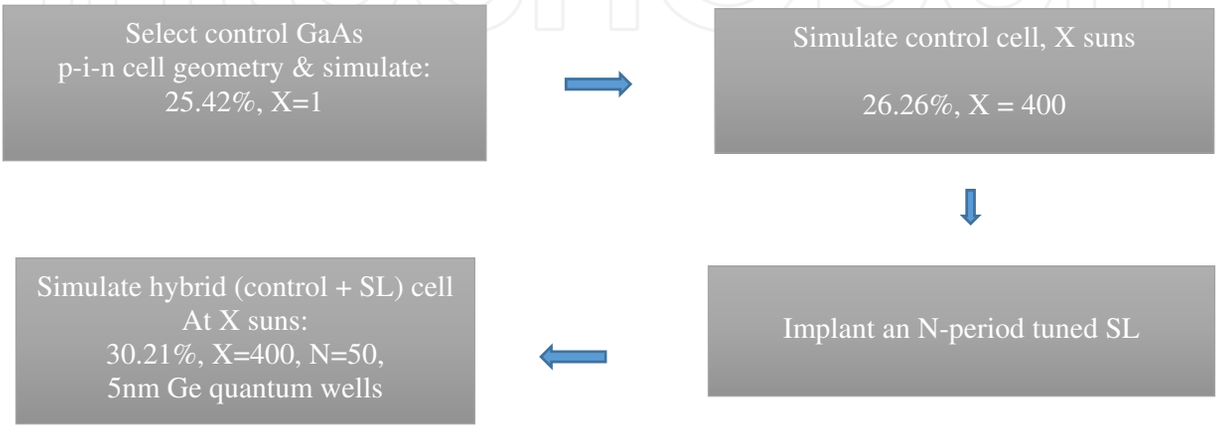

Figure 7. Four steps for hybrid cell simulation

Author details

A.C. Varonides

Physics & Electrical Engineering Dept. University of Scranton, USA

References

[1] www.pveducation.org/pvcdrom/appendices/standard-solar-spectra

[2] RK Pathria, Statistical Mechanics, Pergamon Press, 1972

[3] van der Ziel, Solid State Physical Electronics, Prentice Hall, 1968

[4] O Manasreh, Semiconductor Heterojunctions and Nanostructures, McGraw Hill

[5] S Dimitrijef, Principles of Semiconductors, Oxford U Press 2012

[6] M Shur, GaAs Devices and Circuits, Plenum 1987

[7] AC Varonides, work in progress

[8] H Unlu, A Nussbaum, Band discontinuities as Heterojunction Device Design Parameters, IEEE Transactions on Electron Devices, Vol. ED 33, No 5, May 1986

[9] Capasso/Margaritondo, Heterojunction Band Discontinuities, North Holland 1987

[10] Sze and Lee, Semiconductor Devices, John Wiley, 3d Ed, 2010

[11] PC1D, Version 5.0 (1997) University of New South Wales, Serial # 5034

[12] AC Varonides, Escape rate of thermionic electrons from highly illuminated superlattices, work in progress (EMRS 2015, 30th European PV, 2015)

[13] JM Olson, DJ Friedman, S Kurz, High Efficiency III-V Multijunction Solar Cells, Handbook of Photovoltaic Science and Engineering, Ed. A Luque and S Hegedus, 2003, John Wiley & Sons, Ltd ISBN: 0-471-49196-9

[14] C Algora, Next generation photovoltaics: high efficiency through full spectrum utilization, Marti & Luque editors, Institute of Physics Publ. (Bristol) 2004

[15] DK Ferry, Editor-in-Chief, Gallium Arsenide Technology, Vol II, Howard W. Sams & Company, 1990.

[16] JG Adams, BC Browne et al, Recent results for single-junction and tandem quantum well solar cells, Progress in Photovoltaics Res. Appl., pp 865-877, 2011.

IntechOpen